Research Square

Preprints are preliminary reports that have not undergone peer review.
They should not be considered conclusive, used to inform clinical practice,
or referenced by the media as validated information.

Functional near-infrared spectroscopy reveals ventrolateral prefrontal cortex neural efficiency in instantaneous decision-making by basketball experts

Tian Jiaxing
Harbin Institute of Physical Education
Chang Feng
Harbin Institute of Physical Education
Wang Miao
Harbin Institute of Physical Education
Luo Chunlin
Harbin Institute of Physical Education
Fan Chao
Harbin Institute of Physical Education
Bao Hongbo
Capital Medical University
Liu Mengqi
Harbin Institute of Physical Education
Si Haoqin
Harbin Institute of Physical Education
Zhu Tong
Harbin Institute of Physical Education
Qin Ying
qinyinggaofeng@163.com

Harbin Institute of Physical Education

Article

Keywords: Basketball, Decision-making, Neural efficiency, fNIRS, Cognitive compensation, Spatiotemporal dynamics

Posted Date: July 27th, 2026

DOI: https://doi.org/10.21203/rs.3.rs-10122121/v1

License: This work is licensed under a Creative Commons Attribution 4.0 International License.
Read Full License

Additional Declarations: No competing interests reported.

Abstract

In highly dynamic sports such as basketball, rapid decision-making under extreme time pressure is a hallmark of perceptual-cognitive expertise. Although the neural efficiency hypothesis (NEH) provides a framework for experts' superior performance, its spatiotemporal boundaries in complex tactical contexts remain underexplored. This study examined prefrontal hemodynamics during instantaneous basketball decision-making. Thirty-two participants (16 experts, 16 novices) viewed ecologically valid basketball offensive videos and rapidly predicted the ball-carrier's next move while functional near-infrared spectroscopy (fNIRS) monitored prefrontal hemodynamics across four consecutive task blocks. Behaviorally, experts showed higher decision accuracy and efficiency. Neuroimaging revealed a spatiotemporally specific neural efficiency pattern. Spatially, the expert advantage was localized to lower activation in the ventrolateral prefrontal cortex (VLPFC), with no significant group differences in the dorsolateral prefrontal cortex (DLPFC), suggesting a "resource redirection" strategy that bypasses general cognitive hubs. Experts' VLPFC activation correlated negatively with decision-making efficiency, whereas novices showed a positive correlation, consistent with inefficient cognitive compensation. Temporally, the effect was most pronounced during the mid-task phase (Block 2), after initial cognitive adaptation. These findings extend the NEH by identifying VLPFC-specific spatial pathways and a stage-specific temporal window in basketball decision-making.

Introduction

In open-skill sports such as basketball, the superior performance of expert athletes is reflected not only in highly accurate decision-making but also in exceptional "Decision-making efficiency"–the ability to process information rapidly and accurately in complex tactical situations1–3. This highly efficient translation from perception to action has long been attributed to the neural efficiency hypothesis4. The hypothesis posits that long-term specialized training enables experts to achieve equivalent or superior behavioral performance with lower neural energy expenditure5. However, recent studies indicate that the applicability of the neural efficiency hypothesis (NEH) is not immutable but is significantly modulated by task type6,7. During pure motor execution phases, the NEH generally receives stronger support, manifested as significantly reduced activation in areas such as the motor cortex among experts. Conversely, during judgment phases involving motor imagery or complex tactical cognition, experts' brains sometimes exhibit increased activation in specific regions, a phenomenon known as "neural expansion"8–10. The instantaneous basketball decision-making task employed in this study requires participants to rapidly extract the spatial relationships between offensive and defensive players during a very brief visual exposure (e.g., a 4-second video clip) and to make a tactical judgment (shoot, pass, or drive) via internal representations during the momentary black screen that follows (e.g., within 2 seconds). This process relies heavily on controlled cognitive processing. Therefore, the present study aims to explore whether, under such a high-cognitive-load instantaneous decision paradigm, the neural processing patterns of experts still adhere to the neural efficiency principle. If so, what are the specific boundary conditions for its operation?

To address this paradigm, we argue that the existing theoretical framework requires further extension in both spatial and temporal dimensions. The first is the specificity of spatial distribution. Basketball decision-making is not a simple visual reaction; it demands the filtering of massive amounts of interfering information and the rapid extraction of tactical rules11.Meanwhile, recent studies in orienteering have preliminarily confirmed that highly experienced experts exhibit significantly lower activation in the ventrolateral prefrontal cortex (VLPFC) when executing cognitive tasks, demonstrating a localized neural efficiency characteristic12. Building upon this finding, we propose that neural efficiency in basketball decision-making does not manifest as brain-wide, non-discriminatory global inhibition, but rather as a highly specific "resource redirection." Specifically, experts can inhibit their over-reliance on high-energy-consuming general working memory hubs (e.g., the dorsolateral prefrontal cortex, DLPFC) and instead establish a specific, high-efficiency pathway between the VLPFC–which is responsible for tactical rule extraction and interference inhibition–and primary motor cortex and supplementary motor cortex (e.g., PMC/SMA)13–15. The second dimension is the dynamic nature of the time course. Because continuous video judgment tasks involve task adaptation and the dynamic allocation of cognitive resources, neural efficiency characteristics may not persist throughout the entire task. According to the "neural habituation model"16, individuals are in a phase of paradigm adaptation and strategy exploration during the initial stage of the task (e.g., Block 1), where cognitive load is universally high. After this initial adaptation phase, the experts' automated tactical schemas are successfully activated, at which point the manifestation of neural efficiency may be most pronounced. Subsequently, with the accumulation of fatigue effects, this advantage may undergo dynamic evolution. Motivated by these theoretical considerations and the sport-specific characteristics of basketball, this study utilized basketball set-offense videos with high ecological validity, combining E-Prime and fNIRS technologies, to monitor the instantaneous decision-making performance of basketball experts and novices across consecutive task blocks. The study aimed to test the following hypotheses:

Spatial specificity and brain-behavior pattern validation: To examine the generalizability and specificity of the localized neural efficiency characteristics observed in the VLPFC of highly experienced experts during cognitive tasks, applying them to instantaneous basketball decision-making with a higher cognitive load. We hypothesize that during critical decision-making moments, the expert group will exhibit a more streamlined activation pattern in the VLPFC, and their activation intensity will be negatively correlated with Decision-making efficiency, in accordance with the NEH. Conversely, the novice group will show diffuse and intense VLPFC activation, with a positive correlation between activation intensity and efficiency, demonstrating a phenomenon of neural inefficiency.

Stage dynamics of neural efficiency in instantaneous decision-making: The "high efficiency, low consumption" characteristic of experts exhibits stage specificity. We speculate that significant inter-group differences in neural activation will likely emerge only during the mid-task stage rather than the early task stage. In other blocks, however, experts will maintain a behavioral advantage without significant neural activation differences, relying on specialized schemas consolidated through long-term training.

By revealing the spatiotemporally specific processing characteristics of the VLPFC during instantaneous basketball decision-making, this study transcends previous research that viewed the prefrontal cortex (PFC) as a single, homogeneous functional unit17. Furthermore, it provides temporal (task adaptation stages) and spatial (VLPFC-specific pathways) boundary conditions for the applicability of the NEH in open-skill, complex sports contexts, thereby offering crucial theoretical value and empirical evidence for understanding the dynamic cognitive control models of elite athletes under extreme time pressure.

Results

Behavioral Indicator Test Results

With respect to decision accuracy (ACC), the ACC in Block 1 ($t = 2.26$, $p = .031$, Cohen's $d = 0.80$), Block 2 ($Z = -3.09$, $p = .002$, $r = 0.55$) and the 4th block ($Z = -2.16$, $p = .031$, $r = 0.38$) was significantly greater in the expert group, than in the novice group, while there was no significant difference in the ACC between the groups in block 3 ($Z = -0.71$, $p = .478$). With respect to the reaction rate, there were no significant differences between the two groups in any of the four blocks (all $p > .05$). Crucially, in terms of Decision-making efficiency (DME), the expert group's Decision-making efficiency was significantly greater than that of the novice group in the second block ($Z = -2.07$, $p = .038$, $r = 0.37$). No significant difference in DME was observed in the remaining blocks ($p > .05$). See Fig. 3 for details.

Overall, the behavioral outcome data of the two groups of participants indicate that compared with novices, experts maintained a higher decision-making accuracy rate in the second block of the critical period of the task and achieved higher decision-making efficiency. The detailed data are shown in Table 2.

Table 2
Comparison of behavioral performance between the expert group and the novice group in basketball decision-making tasks (mean ± SD)

Module (Block)	Behavioral indicators	Expert group (*n* = 16)	Novice group (*n* = 16)	*t/Z* value	*p* value	Cohen's *d/r*
Block 1	Accuracy (ACC)	71.43 ± 18.81	56.25 ± 19.14	2.26	.031*	0.80
	Mean Reaction Time (MeanRT)	851.33 ± 190.36	716.58 ± 249.75	1.72	.096	0.61
	Decision-Making Efficiency (DME)	0.08 (0.07, 0.10)	0.08 (0.05, 0.13)	-0.19	.851	0.03
Block 2	Accuracy (ACC)	92.86 (75.00, 100.00)	71.43 (42.86, 85.71)	-3.09	.002**	0.552
	Mean Reaction Time (MeanRT)	836.60 ± 258.79	829.43 ± 317.33	0.07	.945	0.03
	Decision-Making Efficiency (DME)	0.10 (0.08, 0.14)	0.07 (0.06, 0.11)	-2.07	.038*	0.37
Block 3	Accuracy (ACC)	78.57 (71.43, 100.00)	85.71 (71.43, 85.71)	-0.71	.478	0.13
	Mean Reaction Time (MeanRT)	829.16 ± 216.23	743.30 ± 233.55	1.08	.289	0.38
	Decision-Making Efficiency (DME)	0.11 ± 0.03	0.12 ± 0.04	-0.66	.514	-0.23
Block 4	Accuracy (ACC)	85.71 (71.43, 100.00)	71.43 (28.57, 85.71)	-2.16	.031*	0.38
	Mean Reaction Time (MeanRT)	864.61 ± 266.93	747.67 ± 276.75	1.22	.233	0.43
	Decision-Making Efficiency (DME)	0.10 (0.09, 0.14)	0.12 (0.09, 0.15)	0.83	.407	0.15

Note: ACC = decision accuracy; MeanRT = average reaction time; DME = Decision-making efficiency. Indicators conforming to a normal distribution are expressed as the mean ± standard deviation (mean ± SD), and between-group comparisons were performed using an independent samples *t* test, with the effect size reported as Cohen's *d*. Indicators not conforming to a normal distribution are expressed as the median and interquartile range [median (Q1, Q3)], and between-group comparisons were performed using a Mann–Whitney *U* test (corresponding to the *Z* value), with the effect size reported as the r value. * $p < .05$, ** $p < .01$.

Exploratory Analysis of Brain Activation Time Dynamics

To determine the optimal observation window for specialty-specific neural responses and to exclude interference from early task adaptation or late-stage fatigue effects, this study first conducted exploratory intergroup comparisons of HbO activation indices (mean and peak values) covering six regions of interest across all four experimental blocks. For rigor, multiple comparison corrections using the false discovery rate (FDR p) were performed independently for comparisons within each block. The temporal dynamics results across blocks (Table A.1) showed that in the first block, although activation peaks in individual regions (such as the VLPFC and parts of the sensorimotor area) exhibited uncorrected marginal significance ($p < .05$), these were not corrected by FDR p (FDR $p > .05$), suggesting that this was primarily due to nonspecific neural fluctuations during the task adaptation period. As the task progressed to the third and fourth blocks, the subjects may have experienced cognitive fatigue or neural habituation, at which point no significant intergroup differences were observed in any region of interest.

Notably, only in the second block of the critical period of the task did the differences in activation between the expert group and the novice group in the VLPFC and PMC/SMA regions withstand rigorous FDR p correction (FDR $p < .05$). This result not only statistically eliminates the possibility of false positives but also strongly demonstrates that the second block is the “optimal performance window” where subjects’ attention is highly focused and their neural computational strategies are purely displayed. On the basis of this solid exploratory statistical evidence, the comparison of core brain region differences (Table 3) and the targeting mechanism correlation analysis (Table 4) in the main body of this study strictly focus on the data from the second block.

Table 3
Comparison of HbO activation levels between the expert group and the novice group in each region of interest (ROI) of Experiment Module 2 (mean ± SD)

Interest Area (ROI)	**HbO index**	**Expert group (*n* = 16)**	**Novice group (*n* = 16)**	***t/Z* value**	**Original *p* value**	***p* value after FDR correction**	**Cohen's *d/r***
DLPFC	peak	0.227 (0.143, 0.351)	0.246 (0.166, 0.388)	0.42	.678	.836	0.07
	mean	0.103 ± 0.152	0.135 ± 0.141	-0.63	.537	.805	-0.22
VLPFC	peak	0.039 ± 0.186	0.239 ± 0.131	-3.51	.001**	.009**	-1.24
	mean	-0.094 ± 0.193	0.080 ± 0.145	-2.89	.007**	.040*	-1.02
FPA	peak	0.215 (0.150, 0.317)	0.242(0.155,0.356)	0.57	.572	.836	0.10
	mean	0.085 ± 0.216	0.134 ± 0.152	-0.74	.464	.805	-0.26
PMC/SMA	peak	0.058 (0.012, 0.210)	0.150 (0.075, 0.278)	1.92	.055	.110	0.34
	mean	-0.086 ± 0.186	0.068 ± 0.141	-2.63	.013*	.040*	-0.93
OFC	peak	0.228 (0.158, 0.462)	0.214 (0.121, 0.355)	-0.45	.651	.836	-0.08
	mean	0.056 (0.041, 0.140)	0.066 (-0.030, 0.175)	-0.34	.734	.857	-0.06
Other motor sensory areas	peak	0.095 ± 0.123	0.134 ± 0.155	-0.78	.440	.836	-0.28

Note: DLPFC = dorsolateral prefrontal cortex; VLPFC = ventrolateral prefrontal cortex; FPA = frontal pole; PMC/SMA = primary motor cortex and supplementary motor cortex; OFC = orbitofrontal cortex. For HbO concentration changes, those conforming to a normal distribution are expressed as the mean ± standard deviation (mean ± SD) (using an independent samples *t* test, effect size Cohen's *d*); those not conforming to a normal distribution are expressed as the median and interquartile range [median (Q1, Q3)] (using a Mann–Whitney *U* test, effect size r). * $p < .05$, ** $p < .01$ (the significance level here is based on the original *p* value). FDR p correction was performed using the Benjamini–Hochberg method to control for the false-positive rate in multiple comparisons (i.e., the *p* value after FDR correction).

Interest Area (ROI)	HbO index	Expert group (*n* = 16)	Novice group (*n* = 16)	*t/Z* value	Original *p* value	*p* value after FDR correction	Cohen's *d/r*
	mean	-0.011 ± 0.119	0.003 ± 0.168	-0.28	.782	.857	-0.10

Note: DLPFC = dorsolateral prefrontal cortex; VLPFC = ventrolateral prefrontal cortex; FPA = frontal pole; PMC/SMA = primary motor cortex and supplementary motor cortex; OFC = orbitofrontal cortex. For HbO concentration changes, those conforming to a normal distribution are expressed as the mean ± standard deviation (mean ± SD) (using an independent samples *t* test, effect size Cohen's *d*); those not conforming to a normal distribution are expressed as the median and interquartile range [median (Q1, Q3)] (using a Mann–Whitney *U* test, effect size r). * $p < .05$, ** $p < .01$ (the significance level here is based on the original *p* value). FDR p correction was performed using the Benjamini–Hochberg method to control for the false-positive rate in multiple comparisons (i.e., the *p* value after FDR correction).

Table 4
Target correlation analysis of brain activation and decision-making behavior revealing significant intergroup differences in Block 2 between the expert group and the novice group

Grouping	Region of Interest (ROI)	HbO activation index	Behavioral indicators	Correlation analysis methods	Correlation coefficient *r*	Original *p* value
Expert group	VLPFC	peak	Decision accuracy	Spearman rank correlation	− .01	.963
		peak	Decision-making efficiency	Spearman rank correlation	− .57*	.021
		mean	Decision accuracy	Spearman rank correlation	.07	.807
		mean	Decision-making efficiency	Spearman rank correlation	− .54*	.031
	PMC/SMA	mean	Decision accuracy	Spearman rank correlation	.05	.866
		mean	Decision-making efficiency	Spearman rank correlation	− .42	.107
Novice Group	VLPFC	peak	Decision accuracy	Pearson product–moment correlation	.52*	.040
		peak	Decision-making efficiency	Spearman rank correlation	.56*	.024
		mean	Decision accuracy	Pearson product-–moment correlation	.15	0.593
		mean	Decision-making efficiency	Spearman rank correlation	.14	.602

Note: VLPFC = ventrolateral prefrontal cortex; PMC/SMA = primary motor cortex and supplementary motor cortex. In the table, *r* represents the correlation coefficient. On the basis of the normality test results for each group of data, Pearson product–moment correlation analysis (for normally distributed data) or Spearman rank correlation analysis (for nonnormally distributed data) were used to evaluate the associations between HbO activation indicators (peak/mean) and behavioral indicators (decision accuracy/Decision-making efficiency) for each ROI. Given that this correlation analysis is targeted based on significant intergroup main effects, the number of tests was limited; therefore, uncorrected raw *p* values are reported. * $p < .05$.

Grouping	Region of Interest (ROI)	HbO activation index	Behavioral indicators	Correlation analysis methods	Correlation coefficient *r*	Original *p* value
	PMC/SMA	mean	Decision accuracy	Pearson product–moment correlation	.38	.142
		mean	Decision-making efficiency	Spearman rank correlation	.28	.300

Note: VLPFC = ventrolateral prefrontal cortex; PMC/SMA = primary motor cortex and supplementary motor cortex. In the table, *r* represents the correlation coefficient. On the basis of the normality test results for each group of data, Pearson product–moment correlation analysis (for normally distributed data) or Spearman rank correlation analysis (for nonnormally distributed data) were used to evaluate the associations between HbO activation indicators (peak/mean) and behavioral indicators (decision accuracy/Decision-making efficiency) for each ROI. Given that this correlation analysis is targeted based on significant intergroup main effects, the number of tests was limited; therefore, uncorrected raw *p* values are reported. * $p < .05$.

Differences in the activation of core brain regions during the optimal performance period (Block 2)

In the second block of the critical period of the task, the expert group and the novice group showed significant differences in expertise-dependent activation in specific prefrontal and motor cortex brain regions (see Table 3 for details).

First, the Shapiro–Wilk normality test was performed on each HbO index. Indicators conforming to a normal distribution were tested using an independent samples t test, while those not conforming to a normal distribution were tested using the Mann–Whitney U test. To strictly control the false-positive rate, in this study, the “peak value” and “mean value” of HbO were treated as two independent families of hypotheses, and Benjamini–Hochberg FDR p multiple comparison corrections were performed on each.

The results are shown in Fig. 4. In the ventrolateral prefrontal cortex (VLPFC), the characteristic activation in the expert group was significantly lower than that in the novice group. Specifically, the peak HbO activation ($t = -3.51$, original $p = .001$, FDR-corrected $p = .009$, Cohen's $d = -1.24$) and the mean activation level ($t = -2.89$, original $p = .007$, FDR-corrected $p = .040$, Cohen's $d = -1.04$) in the expert group were significantly lower than those in the novice group. Both of these indicators significantly decreased (− 1.02). Both indicators reached the large effect size level ($d > 0.8$), strongly demonstrating that experts can achieve efficient information integration with lower local neural resource consumption when executing complex tactical decisions, resulting in a significant “neural efficiency” characteristic.

Moreover, in the primary motor cortex/supplementary motor area (PMC/SMA), the mean HbO activation level in the expert group was significantly lower than that in the novice group ($t = -2.63$; original $p = .013$; FDR-corrected $p = .040$; Cohen's $d = -0.93$). The peak activation index differed marginally significantly

between the groups (Z = 1.92; original p = .055) but did not significantly differ after strict FDR p correction (FDR-corrected p = .110).

In contrast, no significant differences were observed in activation levels between the two groups in the dorsolateral prefrontal cortex (DLPFC), (FPA), orbitofrontal cortex (OFC), or other motor sensory areas (FDR-corrected p > .05). These findings indicate that neural processing optimization induced by motor expertise is highly region specific, with a primary focus on the VLPFC, which is responsible for rule regulation and conflict inhibition, and the PMC/SMA, which is responsible for action planning. The detailed data are shown in Table 3.

Correlation analysis of specialty-specific brain-behavioral targeting mechanisms

To further elucidate the underlying neural mechanisms through which athletic proficiency influences decision-making performance, this study conducted targeted correlation analysis on core brain regions (the VLPFC and the PMC/SMA) and key behavioral indicators (decision accuracy (ACC) and Decision-making efficiency (DME)) that exhibited significant intergroup main effects in Block 2. Normality was tested, and Pearson product–moment correlation or Spearman rank correlation methods were used. The specific regression coefficients and p values for the correlation tests are shown in Table 4.

The correlation analysis, as shown in Fig. 5, revealed strikingly different neurocognitive mapping patterns between the expert group and the novice group in terms of VLPFC activation and decision-making performance. In the expert group, the core activation index of the VLPFC was significantly negatively correlated with decision-making efficiency (peak: r = − .57, p = .021; mean: r = − .54, p = .031). These results (as shown in Fig. 5) intuitively demonstrate that high-level experts often achieve optimal decision-making efficiency accompanied by relative inhibition of prefrontal cortex control area activation, perfectly confirming the “neural efficiency hypothesis” in expertise development. Conversely, in the novice group, the characteristic activation of the VLPFC was significantly positively correlated with decision-making performance. Specifically, the peak HbO of the VLPFC in the novice group was not only significantly positively correlated with decision accuracy (r = .52, p = .040) but also significantly positively correlated with decision-making efficiency (r = .56, p = .024). As shown by the upward trend line in Fig. 5, novices lack automated processing schemas when faced with complex visual situations and must allocate more prefrontal cognitive resources from top to bottom to compensate for their insufficient abilities. Furthermore, no statistically significant correlations were detected between activation levels in the primary motor cortex/supplementary motor area (PMC/SMA) and any behavioral indicators in either group (all p > .05). This trend indicates that within the expert group, lower activation is associated with higher decision-making efficiency (negative correlation), whereas the novice group exhibits higher activation and higher decision-making efficiency (positive correlation).

Discussion

Overview of principal findings

Utilizing a basketball instantaneous decision-making paradigm with high ecological validity, this study investigated the behavioral performance and prefrontal hemodynamic responses of experts and novices across consecutive tasks. The results demonstrated that the expert group exhibited significant advantages in both decision accuracy and Decision-making efficiency, further corroborating the generalizability of the Neural Efficiency Hypothesis to open-skill sports at the behavioral level27,28. More importantly, this study provided specific spatial and temporal boundary conditions for the NEH at the neuroimaging level. Our data indicate that neural efficiency is not a static, global brain functional characteristic but rather a dynamic equilibrium process jointly constrained by specific brain regions (spatial dimension) and task stages (temporal dimension). This finding not only challenges the traditional generalized perception of "high efficiency" within the NEH but also delineates the applicability of previous findings across different sports, thereby supplementing crucial boundary conditions for understanding the cognitive control mechanisms of elite athletes under pressure.

Spatial specificity of neural efficiency

In the spatial dimension, this study observed a significant "functional segregation" phenomenon. Unlike early studies that found a "global decrease in prefrontal activation"29, the present study revealed that the efficiency advantage of the expert group was precisely localized to the ventrolateral prefrontal cortex (VLPFC), whereas activation in the dorsolateral prefrontal cortex (DLPFC) showed no significant inter-group differences. This result is highly consistent with recent findings in orienteering research, strongly validating the cross-sport generalizability of the VLPFC as a core neural indicator of sports expertise12.

This spatial specificity reflects the "resource redirection" strategy of the expert brain in basketball30. The DLPFC typically governs general, high-energy-consuming working memory maintenance, whereas the VLPFC focuses on specific tactical rule extraction and interference inhibition. Relying on long-term specialized training, experts have formed automated tactical schemas, enabling them to establish a precise "processing shortcut" via the VLPFC, thereby inhibiting over-reliance on general cognitive hubs. Targeted correlation analysis provided empirical support for this deduction: the significant negative correlation ($r = -0.57$) between VLPFC activation and efficiency in the expert group verified the NEH logic. Conversely, the positive correlation ($r = 0.56$) in the novice group revealed that, due to a lack of experience, novices engaged in compensatory recruitment when facing complex tactics, attempting to complete the task through cognitive compensation. However, lacking automated schemas, this forced cognitive investment ultimately manifested as a typical "neural inefficiency" phenomenon31,32.

The temporal dynamics of neural efficiency

In the temporal dimension, this study transcended previous static descriptions of the NEH, finding that inter-group differences in VLPFC activation were not present throughout the entire experiment but were

primarily concentrated in a specific mid-task window (Block 2). This result suggests that when processing complex, open-skill sports situations like basketball, the manifestation of neural efficiency may possess significant time-dynamic characteristics rather than being immutable33.

Combined with the neural habituation model, this stage-specific manifestation may be related to the high information complexity of basketball and the individuals' task adaptation process. During the initial task stage (Block 1), due to the novel paradigm and dense tactical interference information, both experts and novices likely consumed significant cognitive resources to adapt to the testing requirements, resulting in underlying neural efficiency differences that were not macroscopically prominent in hemodynamics. However, after overcoming the initial "adaptation costs" (Block 2), the experts' mature specialized schemas were successfully engaged, revealing the relative "high efficiency, low consumption" advantage in localized brain regions. The flattening of group differences in the later stages (Blocks 3/4) may have been influenced by a combination of complex factors, such as cognitive fatigue induced by continuous judgments or short-term learning effects in novices34–38.

Furthermore, although current constraints on sample size and the macroscopic temporal resolution of fNIRS prevent definitive conclusions regarding the underlying rapid electrophysiological mechanisms, the block-wise fluctuations observed in this study may indirectly reflect the dynamic "rhythmic reorganization" of cortical networks within specific time windows39,40. These preliminary findings provide valuable empirical clues for decoding how elite athletes dynamically allocate cognitive resources as a task progresses and highlight the need for future large-sample studies to focus on the modulatory effects of task stages on neural efficiency.

Practical implications for talent identification and cognitive training

The preliminary findings of this study offer novel perspectives for scientific training and talent identification in open-skill competitive sports. First, the assessment of tactical ability should gradually shift from a purely "result-oriented" to an "efficiency-oriented" approach. The study suggests that when selecting or evaluating elite athletes, assessments should not be limited to the accuracy of explicit behaviors; future practices could consider integrating the neurophysiological expenditure of localized brain regions (e.g., VLPFC) as an auxiliary monitoring metric. This dual "brain-behavior" assessment model could help identify elite athletes who genuinely possess automated tactical schemas in complex, high-pressure situations41,42.

Second, the time-dynamic characteristic of neural efficiency provides empirical grounding for implementing pre-match "cognitive warm-ups." Given the universally present cognitive adaptation costs during the initial phase of high-load tasks (as shown by Block 1 performance in this study), coaching teams could attempt to introduce tactical video previews or virtual environment simulations of specific intensities alongside conventional physical warm-ups43. This cognitive pre-activation strategy holds the potential to help athletes bypass the initial high-resource-consumption phase, enabling their brain

networks to rapidly enter an "optimal engagement period" (similar to Block 2) at the starting whistle, thereby seizing the decision-making initiative in the ever-changing early stages of a match.

Although this study provides new empirical clues for the neurodynamic mechanisms of instantaneous basketball decision-making, several limitations point the way for future in-depth research.

Limitations

First is the trade-off between internal and ecological validity. Constrained by the optical acquisition requirements and motion artifact sensitivity of conventional fNIRS equipment, participants in this study were required to complete button-press responses in a relatively stationary seated position. While this design strictly controlled for extraneous variables, it somewhat stripped away the embodied characteristics of "perception-action coupling" present in real sports arenas44,45. Future studies could consider employing artifact-resistant, portable, wireless wearable fNIRS systems combined with virtual reality (VR) technology to further examine the spatiotemporal dynamics of neural efficiency during actual physical movement.

Second is the limitation regarding sample size and demographic distribution. As established by our sensitivity power analysis, the achieved sample (n = 16 per group) was sufficient to detect large between-group differences ($d \geq 1.02$ at 80% power), corresponding to the magnitude of the VLPFC effects observed in the present study (peak HbO Cohen's d = 1.24; mean HbO Cohen's d = 1.24). However, the sample was statistically underpowered for detecting medium effects ($d \leq 0.7$). Consequently, the absence of significant group differences in regions such as the DLPFC, FPA, and OFC should not be interpreted as definitive evidence for null effects. Future replication studies aiming to establish neural specificity with greater confidence should target a minimum of approximately 26 participants per group (calculated for $d = 0.7$ at $\alpha = 0.05$, two-tailed, 80% power) to robustly distinguish trueregional specificity from Type II error.

Lastly is the compromise in the temporal resolution of neuroimaging techniques. fNIRS signals primarily reflect slow hemodynamic changes in cortical blood oxygenation and struggle to directly capture high-frequency neural oscillations and instantaneous electrophysiological connectivity within brain networks46. Given the irreplaceable role of millisecond-level processing windows (e.g., 0-200 ms instantaneous perception and feature extraction) and high-frequency EEG rhythms (e.g., alpha/mu rhythm desynchronization) in fully decoding decision-making mechanisms, future research should strongly consider introducing simultaneous fNIRS-EEG multimodal acquisition technologies47. Achieving deep complementarity between high spatial localization and high temporal resolution will systematically decipher the underlying "neurovascular coupling" mechanisms of the brain during instantaneous high-pressure decisions, thereby constructing a comprehensive dynamic cognitive control model ranging from microscopic millisecond rhythms to macroscopic localized hemodynamic reorganization.

Conclusion

In complex, dynamic decision-making contexts, the expert group not only maintained higher anticipation accuracy but also demonstrated superior overall Decision-making efficiency. This finding, to some extent, corroborates the positive shaping of higher-order cognitive processing capacities through long-term specialized training.

The ventrolateral prefrontal cortex (VLPFC) is likely a critical brain region for distinguishing cognitive expertise in basketball. During the decision-making process, rather than exhibiting brain-wide, diffuse inhibition, the expert group established a more specific processing pathway in the VLPFC by reducing over-reliance on general cognitive hubs (DLPFC). The divergent patterns between the two groups regarding VLPFC activation and behavioral efficiency provide empirical evidence for the localized manifestation of the Neural Efficiency Hypothesis within this specific sport.

Neural efficiency characteristics exhibit genuine dynamic variations, which, in the context of basketball, specifically manifest after the initial task adaptation phase. This indicates that under the extremely high cognitive loads of complex sports decision-making, the "high efficiency, low consumption" trait of experts is not a persistent static state but rather a dynamic equilibrium strictly modulated by task load and adaptation stages.

Materials and Methods

Participants

Considering the common motion artifacts and data quality risks in functional near-infrared spectroscopy (fNIRS) experiments, this study employed an over-recruitment strategy. Initial recruitment targeted 42 participants (21 per group) based on anticipated effect sizes from prior fNIRS investigations of expertise-related neural efficiency in athletes. However, owing to the difficulty of recruiting elite basketball athletes, 40 participants (20 per group) were ultimately enrolled. During data preprocessing, 8 participants were further excluded based on predefined quality control criteria: 3 participants whose decision-making accuracy fell below the chance level, and 5 participants whose fNIRS signals exhibited uncorrectable severe motion artifacts. The final analytic sample therefore comprised 32 participants (expert group n = 16; novice group n = 16). To evaluate the statistical sensitivity of this final sample, a sensitivity power analysis was conducted using G*Power 3.1.9.718. With $\alpha = 0.05$ and statistical power $(1 - \beta) = 0.80$ for a two-tailed independent- samples t-test, the analysis indicated that the minimum detectable effect size for the present sample was Cohen's $d = 1.024$ (noncentrality parameter $\delta = 2.895$; critical $t = 2.042$; $df = 30$). This indicates that the present study was adequately powered to detect large between-group effects ($d \geq 1.02$), which is consistent with the magnitudes of expertise-related neural efficiency effects reported in prior fNIRS research on athletes12. However, the sample provided limited sensitivity for detecting medium-magnitude effects ($d \leq 0.7$) reported in broader meta-analyses of neural efficiency9. Accordingly, all non-significant findings (e.g., in the DLPFC, FPA, and OFC) are interpreted with appropriate caution, as they may reflect either true null effects or insufficient sensitivity to medium-magnitude differences. All the subjects reported good overall health, normal or corrected vision, normal

color vision, and no history of neurological diseases, mental illnesses, or brain injuries and were right-handed. Subjects were instructed to abstain from alcohol and drugs and did not have insomnia within 24 hours before the experiment. They were divided into two groups on the basis of their basketball training background (demographic characteristics are detailed in Table 1).

Table 1
Comparison of participants' demographic characteristics and specific experience (mean ± SD)

Index	Expert group (n = 16)	Novice group (n = 16)	t/Z value	p value
Age (years)	23.31 ± 1.14	23.00 ± 1.41	0.69	.496
Height (cm)	179.94 ± 6.48	176.75 ± 7.03	1.33	.192
Weight (kg)	72.13 ± 8.85	73.06 ± 9.19	-0.29	.771
BMI (kg/m²)	22.22 ± 1.89	23.31 ± 1.82	-1.66	.108
Specialized training duration (years)	5.00 (4.00, 5.50)	1.00 (0.00, 1.75)	-4.64	< .001***

Note: BMI = body mass index. Continuous variables that conformed to a normal distribution (age, height, weight, and BMI) are expressed as the mean ± standard deviation (mean ± SD), and comparisons between groups were performed using an independent samples t test (corresponding to the t value). Variables that did not conform to a normal distribution (years of specialized training) are expressed as the median and interquartile range [median (Q1, Q3)], and comparisons between groups were performed using the Mann–Whitney U test (corresponding to the Z value). p < .001.

The expert group (n = 16; 13 males, 3 females) consisted of basketball team members and specialized students from Harbin Sport University who possessed systematic competitive experience, with a median of 5.00 years of specialized training (IQR: 4.00, 5.50). Owing to the intensive training and competition schedules of high-level elite athletes and actual recruitment conditions (such as some eligible male team members being unable to participate because of training conflicts), this group was supplemented with active female team members of an equivalent competitive level during recruitment. The novice group (n = 16; 11 males, 5 females) consisted of ordinary college students with no prior basketball training experience, with a median of 1.00 year of specialized training (IQR: 0.00, 1.75). Statistical analysis revealed that the two groups were similar in terms of age (p = .496), height (p = .192), weight (p = .771) and BMI (p = .108), and the baseline was well matched; however, there were extremely significant differences in the number of years of specialized training (Z = − 4.64, p < .001), ensuring the validity of the grouping.

Experimental Materials and Methods

This study employed a temporal occlusion paradigm to assess athletes' predictive abilities. This paradigm requires participants to react when watching a video recording of a game up to a critical decision point (e.g., before a pass), at which point subsequent visual information is interrupted 19. Previous research has demonstrated that skilled athletes can accurately predict events using kinematic cues in the very early stages of movement execution (e.g., 80 ms before ball contact)20. Therefore, the

3–5 second video clips used in this experiment are sufficient to cover the complete kinematic information flow from the initiation of the movement to the occurrence of the critical event, conforming to the standard design of this paradigm and effectively examining the differences between expert and novice groups in utilizing early kinematic cues. Furthermore, the 45 high-definition video clips used in this experiment were all sourced from official top-level international events organized by the International Basketball Federation (FIBA) and the International Olympic Committee (IOC)21. The video footage was primarily taken from basketball matches at the 2024 Paris Olympics (such as the Men's Group C match between Serbia and the USA), the 2023 FIBA Basketball World Cup, the 2022 FIBA Women's Basketball World Cup, and the 2020 Tokyo Olympics. All the videos consist of real-world set pieces with complex tactical plays and high cognitive demands. To eliminate irrelevant variables, all videos were evaluated and selected by two basketball coaches with national-level or higher qualifications. Professional video editing software (such as EV Screen Recorder) was used to standardize and trim the original videos, removing audio, scoreboards, and replay footage.

Experimental Procedure

The experiment consisted of a practice phase and a formal testing phase. The practice phase included four trials for practice, and the stimulus materials used in this phase did not reappear in the subsequent formal testing phase. The purpose of this phase was to help participants familiarize themselves with the experimental task requirements, and no data were collected during this period.

Thirty seconds of resting-state data were collected first and served as the baseline data. At the start of the experiment, a red fixation point symbol “+” was first displayed on a white background for 1 second, followed by a 4-second video clip of a ball being served (the video clips were played randomly and without repetition); then, the screen turned black for 2 seconds. During this blackout period, participants were required to quickly judge the ball handler's next decision (pass, shoot, or drive) and press the corresponding number on the keyboard (1 for pass, 2 for shoot, or 3 for drive). If a participant did not respond within 2000 ms or pressed a key after the start of the next trial, that trial was recorded as missing data or an invalid response. Then, the program automatically moved to the next trial. Every seven trials constituted a block. After the task of each block was completed, a 30-second rest period was given. The entire experiment included 4 blocks and a total of 28 formal trials (excluding the 4 trials in the practice phase). To make the scenario as realistic as possible, the participants needed to make a judgment within 2 seconds of the black screen. Judgments that exceeded the time limit were not included in the subsequent statistical analysis. The experimental testing process is shown in Fig. 1.

Experimental Equipment

fNIRS equipment

The fNIRS data for this study were acquired using a BS-7000 near-infrared spectroscopy system (Wuhan Zilian Hongkang Technology Co., Ltd., Wuhan, China). This system uses dual-wavelength laser diodes (690 nm and 830 nm) to measure changes in cortical hemoglobin concentration at a sampling frequency

of 20 Hz. The experiment employed 15 emitters and 15 detectors, resulting in the formation of 47 data acquisition channels. Each channel consisted of an emitter–detector pair spaced approximately 3 cm apart to ensure that the detection depth reached the gray matter cortex of the brain.

The arrangement of the photoelectric caps followed the internationally accepted 10–20 EEG positioning system, with the transmitter S1 corresponding to the Fpz point and the Cz point (top of the head) serving as the central reference point. To accurately locate anatomical brain regions, the spatial three-dimensional coordinates of the reference points (Nz, Cz, AL, and RL) and all photoelectric poles were recorded using a 3D positioning device (NirMap, Wuhan Zilian Hongkang Technology Co., Ltd., Wuhan, China).

Spatial localization was performed using the NIRS-SPM method, which is based on the international 10–20 system and maps the measurement location to the standard MNI space22. Forty-seven channels were accurately projected onto the cortical surface and first matched to the corresponding Brodmann areas (BAs). To subsequently align with the executive control and motor intention networks explored in this study and to improve the spatial specificity and signal-to-noise ratio of the signals, adjacent and functionally related channels were combined, ultimately dividing the area into six core regions of interest (ROIs). This ROI division method referenced established practices for functional grouping of channels based on Brodmann areas23. Specifically, these include the DLPFC, VLPFC, FPA, PMC/SMA, OFC, and other motor/sensory areas. The specific 2D channel arrangement matrix, 3D spatial projection of the brain region, and details of the channels included in each ROI are shown in Fig. 2.

Equipment for recording behavioral indicators

The presentation of behavioral stimuli (basketball video footage) and the acquisition of key response data in this study were both completed using E-Prime 3.0.10 software (Psychology Software Tools, Pittsburgh, PA, USA). Experimental tests were conducted on a portable computer equipped with a 15.6-inch LCD monitor (60 Hz refresh rate, 1920×1080 resolution), with all video stimuli presented in full-screen, centered mode.

During the experiment, participants sat comfortably in a quiet, dark laboratory, with their eyes level with the center of the screen and a viewing distance of approximately 60 cm. When performing a basketball decision-making task, participants responded quickly using the number keys (“1”, “2”, and “3”) on a standard computer keyboard. E-Prime software synchronously and precisely recorded the participants’ key selections and reaction times (RTs) for each decision in the background, with hardware precision down to the millisecond (ms) level. These data served as the primary behavioral data for subsequent calculations of decision accuracy (ACC) and overall Decision-making efficiency (DME).

Synchronization Recording Method

In this study, precise time synchronization of behavioral data (recorded by E-Prime 3.0) and cerebral hemodynamic data (recorded by fNIRS) was achieved using a TCP/IP communication protocol based on

a local area network (LAN).

In terms of hardware connectivity, both the stimulus presentation portable computer and the fNIRS display and control computer were connected to the same gigabit network switch via standard Ethernet cables, creating a closed and stable local area network environment. To ensure the absolute reliability of network communication, the IPv4 protocols of both devices were configured with fixed static IP addresses in the same network segment (set to the 192.168.9.x network segment in this study).

In the actual data acquisition and joint activation process, the experimenter first completed the subject information registration and photoelectric signal quality calibration in the fNIRS acquisition system and then switched the fNIRS system to the managed standby mode of “Wait for External Trigger”. On the E-Prime master control unit, the corresponding IP address and port number were preset through the network communication interface (Socketobject) called internally by the program. When E-Prime officially started the experimental test (covering the practice phase before the formal experiment), the master computer automatically sent an initial activation signal to the fNIRS device via the local area network, instantly waking up the fNIRS system and simultaneously starting continuous recording of whole-brain hemodynamic data.

Throughout the experimental paradigm, the E-Prime program automatically wrote digital event markers into the fNIRS data stream at precise timeframes at the start of the remaining periods for the four decision task blocks. These latency-free hard-triggered markers served as crucial temporal anchors, providing a reliable basis for the precise offline timeline alignment of continuous brain functional signals with specific behavioral decision tasks during later data analysis.

Data Statistics and Analysis

Behavioral Data Preprocessing

The original behavioral data were automatically recorded in the background using E-Prime 3.0 software (Psychology Software Tools, Sharpsburg, PA, USA). After the data collection was completed, the data of all the subjects were merged and initially extracted using E-DataAid 3 and E-Merge 3 software and then exported to Microsoft Excel for centralized calculation. For each test block, the following core behavioral indicators were extracted: (1) decision accuracy (ACC), which was calculated by dividing the number of correct responses in the block by the total number of responses in the block; (2) mean reaction time (MeanRT), to eliminate interference from extreme reactions, premature button presses or inattention, only valid responses with correct responses within the range of 200 ms to 2000 ms were selected for average calculation; (3) Decision-making efficiency (DME), as a core derivative indicator that comprehensively considers speed and accuracy, was calculated according to the unified formula DME = ACC/MeanRT. This indicator has good validity for distinguishing decision performance at different skill levels24.

Preprocessing of fNIRS Data

Offline preprocessing and targeted feature extraction of fNIRS data were performed using NirMaster neuroimaging analysis software. Because oxyhemoglobin (HbO) is highly sensitive to changes in cortical hemodynamics and cognitive load, in this study, HbO concentration changes were selected as the core neurophysiological indicator 25. The specific preprocessing procedure is as follows: First, to reduce the computational load and remove high-frequency noise, the original optical density signal acquired at 20 Hz was resampled to 10 Hz. Then, signal quality control was performed, using the coefficient of variation (CV) to evaluate the channel signals, and channels with a CV value exceeding 20% were removed. For motion artifacts, the system used an automatic identification and correction algorithm (parameter settings: tMotion = 0.5, STDEVthresh = 20, tMask = 3, and AMPthresh = 5). Next, an infinite impulse response (IIR) bandpass filter was used to filter the signal (cutoff frequency set to 0.01 Hz ~ 0.25 Hz) to remove physiological noise such as heartbeat and respiration, as well as instrument baseline drift, and linear detrending was performed. The modified Beer–Lambert law (MBLL) was used to convert optical density into changes in hemoglobin concentration. In the block averaging phase, on the basis of the temporal structure of the experimental paradigm (including a 30-second rest period and an approximately 50-second task period), a time window from 10 seconds before the marker to 80 second after (− 10 s ~ 80 s) was selected as the complete analysis interval, and baseline calibration (baseline correction) was strictly performed using the interval mean of the first 10 seconds (− 10 s ~ − 0.1 s). After the above steps, the peak and mean HbO values for each subject within a specific region of interest (ROI) were extracted for subsequent statistical analysis.

Statistical Analysis

Preprocessed behavioral indicators were combined with the HbO index from fNIRS to construct a subject-level dataset, which was then imported into IBM SPSS Statistics 27.0 (IBM Corp, Armonk, NY, USA) for comprehensive statistical inference. First, the Shapiro–Wilk test was used to test the normality of all the continuous variables. For normally distributed variables, the independent samples t test was used to assess the intergroup difference between the expert group and the novice group, and Cohen's d was reported as the effect size. For nonnormally distributed data, the nonparametric Mann–Whitney U test was used, and r was reported as the effect size. To address the spatial multiple comparisons caused by the multichannel and multiregional nature of fNIRS, all intergroup comparisons of brain activation intensity in this study were corrected for with a strict false discovery rate (FDR p) ($p < .05$)26. Finally, to explore the intrinsic link between brain function and overt behavioral performance, Pearson or Spearman correlation analysis (depending on the normality of the data) was used to examine the correlation between peak HbO levels in target brain regions (such as the VLPFC) and core behavioral indicators (ACC and DME). The two-sided significance level for all the statistical tests was set at $p < .05$. After the intergroup difference in brain activation was analyzed with multiple comparison correction (FDR p), to further reveal the coupled relationship between neural characteristics and overt behavioral performance, the HbO activation values of core brain regions (the VLPFC and the PMC/SMA) that showed significant intergroup main effects were extracted, and targeted correlation analysis with decision accuracy and Decision-making efficiency was performed. Considering that this analysis is based on prior significance results and strictly limits the comparison dimensions, to avoid Type II errors

caused by overpunishment, the correlation analysis reported only the uncorrected raw p values (significance level set at α = 0.05).

Declarations

Ethical Approval

The study was conducted in accordance with the Declaration of Helsinki and was approved by the Institutional Review Board (or Ethics Committee) of Harbin Institute of Physical Education (No. 2026044).

Informed Consent

Written informed consent was obtained from all individual participants included in the study.

Additional Information

Competing interests

The authors declare no competing interests.

Funding

This work was supported by the Natural Science Foundation of Heilongjiang Province (Grant No. LH2024C063).

Author Contribution

A Literature review, manuscript preparation; G Experimental procedures, data analysis; H Experimental procedures; D Experimental procedures, data collection; I Data collection; C Project supervision; B Project supervision, experimental design; E Experimental design; J Theoretical guidance, initial review and revision of the manuscript; F Theoretical guidance, initial review and revision of the manuscript.

Data Availability

The datasets generated during and/or analyzed during the current study are available from the corresponding author on reasonable request.

References

1. Mann, D. T. Y., Williams, A. M., Ward, P. & Janelle, C. M. Perceptual-Cognitive Expertise in Sport: A Meta-Analysis. *J. Sport Exerc. Psychol.* **29**, 457–478 (2007).
2. Travassos, B. et al. Expertise effects on decision-making in sport are constrained by requisite response behaviours – A meta-analysis. *Psychol. Sport Exerc.* **14**, 211–219 (2013).
3. Gou, Q. & Li, S. The influence of basketball players' tracking speed ability on sports decision performance. *PeerJ* **13**, e20266 (2025).
4. Li, L. & Smith, D. M. Neural Efficiency in Athletes: A Systematic Review. *Front. Behav. Neurosci.* **15**, 698555 (2021).
5. Neubauer, A. C. & Fink, A. Intelligence and neural efficiency. *Neurosci. Biobehav Rev.* **33**, 1004–1023 (2009).
6. Gkintoni, E., Sortwell, A. & Vantarakis, A. Neural Efficiency and Sensorimotor Adaptations in Swimming Athletes: A Systematic Review of Neuroimaging and Cognitive–Behavioral Evidence for Performance and Wellbeing. *Brain Sci.* **16**, 116 (2026).
7. Yin, J., Yang, K., Zhou, C. & Dang, J. Motor expertise modulates cortical activation during imagery of simple and complex actions. *Proc. Natl. Acad. Sci.* 122, e2515027122 (2025).
8. Causse, M., Chua, Z., Peysakhovich, V., Del Campo, N. & Matton, N. Mental workload and neural efficiency quantified in the prefrontal cortex using fNIRS. *Sci. Rep.* **7**, 5222 (2017).
9. Filho, E., Dobersek, U. & Husselman, T. A. The role of neural efficiency, transient hypofrontality and neural proficiency in optimal performance in self-paced sports: a meta-analytic review. *Exp. Brain Res.* **239**, 1381–1393 (2021).
10. Swann, C., Moran, A. & Piggott, D. Defining elite athletes: Issues in the study of expert performance in sport psychology. *Psychol. Sport Exerc.* **16**, 3–14 (2015).
11. Balish, S. M., McLaren, C., Rainham, D. & Blanchard, C. Correlates of youth sport attrition: A review and future directions. *Psychol. Sport Exerc.* **15**, 429–439 (2014).
12. Liu, J., Liu, Y. & Wu, L. Exploring the dynamics of prefrontal cortex in the interaction between orienteering experience and cognitive performance by fNIRS. *Sci. Rep.* **14**, 14918 (2024).
13. Gusnard, D. A. & Raichle, M. E. Searching for a baseline: Functional imaging and the resting human brain. *Nat. Rev. Neurosci.* **2**, 685–694 (2001).
14. Miller, E. K. & Cohen, J. D. An Integrative Theory of Prefrontal Cortex Function. *Annu. Rev. Neurosci.* **24**, 167–202 (2001).
15. Smith, S. M. et al. Resting-state fMRI in the Human Connectome Project. *NeuroImage* 80, 144–168 (2013).
16. Huber, D. E., Tian, X., Curran, T., O'Reilly, R. C. & Woroch, B. The dynamics of integration and separation: ERP, MEG, and neural network studies of immediate repetition effects. *J. Exp. Psychol. Hum. Percept. Perform.* **34**, 1389–1416 (2008).
17. Vartanian, L. R., Wharton, C. M. & Green, E. B. Appearance vs. health motives for exercise and for weight loss. *Psychol. Sport Exerc.* **13**, 251–256 (2012).

18. Faul, F., Erdfelder, E., Lang, A. G. & Buchner, A. G*Power 3: A flexible statistical power analysis program for the social, behavioral, and biomedical sciences. *Behav. Res. Methods*. **39**, 175–191 (2007).
19. Discombe, R. M. et al. Effects of traditional and immersive video on anticipation in cricket: A temporal occlusion study. *Psychol. Sport Exerc.* **58**, 102088 (2022).
20. Li, Y. & Feng, T. The Effect of Judgement Bias on Cue Utilization for Shot Prediction in Basketball Athletes. *Brain Sci.* **11**, 1058 (2021).
21. Belling, P. K., Suss, J. & Ward, P. Advancing theory and application of cognitive research in sport: Using representative tasks to explain and predict skilled anticipation, decision-making, and option-generation behavior. *Psychol. Sport Exerc.* **16**, 45–59 (2015).
22. Zang, Y., Jiang, T., Lu, Y., He, Y. & Tian, L. Regional homogeneity approach to fMRI data analysis. *NeuroImage* 22, 394–400 (2004).
23. Zou, J., Yin, Y., Lin, Z. & Gong, Y. The analysis of brain functional connectivity of post-stroke cognitive impairment patients: an fNIRS study. *Front. Neurosci.* **17**, 1168773 (2023).
24. Tang, W., Chen, S., Lin, Y. & Xue, C. Image Entropy-Based Interface Evaluation Method for Nuclear Power Plants. *Entropy* **25**, 1636 (2023).
25. Huang, J. et al. Predicting N2pc from anticipatory HbO activity during sustained visuospatial attention: A concurrent fNIRS–ERP study. *NeuroImage* **113**, 225–234 (2015).
26. Benjamini, Y. & Hochberg, Y. Controlling the False Discovery Rate: A Practical and Powerful Approach to Multiple Testing. *J. R Stat. Soc. Ser. B Stat. Methodol.* **57**, 289–300 (1995).
27. Gao, Q. & Zhang, L. Brief mindfulness meditation intervention improves attentional control of athletes in virtual reality shooting competition: Evidence from fNIRS and eye tracking. *Psychol. Sport Exerc.* **69**, 102477 (2023).
28. Wang, S. & Lu, S. Brain Functional Connectivity in the Resting State and the Exercise State in Elite Tai Chi Chuan Athletes: An fNIRS Study. *Front. Hum. Neurosci.* **16**, 913108 (2022).
29. Haier, R. J. et al. Cortical glucose metabolic rate correlates of abstract reasoning and attention studied with positron emission tomography. *Intelligence* **12**, 199–217 (1988).
30. Eysenck, M. W., Derakshan, N., Santos, R. & Calvo, M. G. Anxiety and cognitive performance: Attentional control theory. *Emotion* **7**, 336–353 (2007).
31. Park, D. C. & Reuter-Lorenz, P. The Adaptive Brain: Aging and Neurocognitive Scaffolding. *Annu. Rev. Psychol.* **60**, 173–196 (2009).
32. Reuter-Lorenz, P. A. & Cappell, K. A. Neurocognitive Aging and the Compensation Hypothesis. *Curr. Dir. Psychol. Sci.* **17**, 177–182 (2008).
33. Li, R. et al. Concurrent fNIRS and EEG for Brain Function Investigation: A Systematic, Methodology-Focused Review. *Sensors* **22**, 5865 (2022).
34. Dayan, E. & Cohen, L. G. Neuroplasticity Subserving Motor Skill Learning. *Neuron* **72**, 443–454 (2011).

35. Klatt, S. & Smeeton, N. J. Processing visual information in elite junior soccer players: Effects of chronological age and training experience on visual perception, attention, and decision making. *Eur. J. Sport Sci.* **22**, 600–609 (2022).
36. Marcora, S. M., Staiano, W. & Manning, V. Mental fatigue impairs physical performance in humans. *J. Appl. Physiol.* **106**, 857–864 (2009).
37. Oka, N. & Asgher, U. Changes in Prefrontal Cortex and Skeletal Muscle Metabolism Associated with Muscle Fatigue: An FNIRS Study. in Advances in Neuroergonomics and Cognitive Engineering (eds (eds Ayaz, H. & Asgher, U.) vol. 1201 238–244 (Springer International Publishing, Cham, (2021).
38. Yan, Y., Guo, Y. & Zhou, D. Mental fatigue causes significant activation of the prefrontal cortex: A systematic review and meta-analysis of fNIRS studies. *Psychophysiology* **62**, e14747 (2025).
39. Stitt, I. et al. Dynamic reconfiguration of cortical functional connectivity across brain states. *Sci. Rep.* **7**, 8797 (2017).
40. Ter Wal, M. et al. Theta rhythmicity governs human behavior and hippocampal signals during memory-dependent tasks. *Nat. Commun.* **12**, 7048 (2021).
41. di Fronso, S. et al. Neural Markers of Performance States in an Olympic Athlete: An EEG Case Study in Air-Pistol Shooting. *J. Sports Sci. Med.* **15**, 214–222 (2016).
42. Shen, Q. Q. et al. Exercise promotes brain health: a systematic review of fNIRS studies. *Front. Psychol.* **15**, 1327822 (2024).
43. Richlan, F., Weiß, M., Kastner, P. & Braid, J. Virtual training, real effects: a narrative review on sports performance enhancement through interventions in virtual reality. *Front. Psychol.* **14**, 1240790 (2023).
44. Araújo, D., Davids, K. & Hristovski, R. The ecological dynamics of decision making in sport. *Psychol. Sport Exerc.* **7**, 653–676 (2006).
45. Vignais, N. et al. Virtual Environments for Sport Analysis: Perception-Action Coupling in Handball Goalkeeping. *Int. J. Virtual Real.* **8**, 43–48 (2009).
46. Tak, S. & Ye, J. C. Statistical analysis of fNIRS data: a comprehensive review. *NeuroImage 85 Pt*. **1**, 72–91 (2014).
47. Pinti, P., Tachtsidis, I., Burgess, P. W. & Hamilton, A. F. D. C. Non-invasive optical imaging of brain function with fNIRS: Current status and way forward. *Encyclopedia Hum. Brain*. (Elsevier), 96–120. 10.1016/B978-0-12-820480-1.00028-0 (2025).

Figures

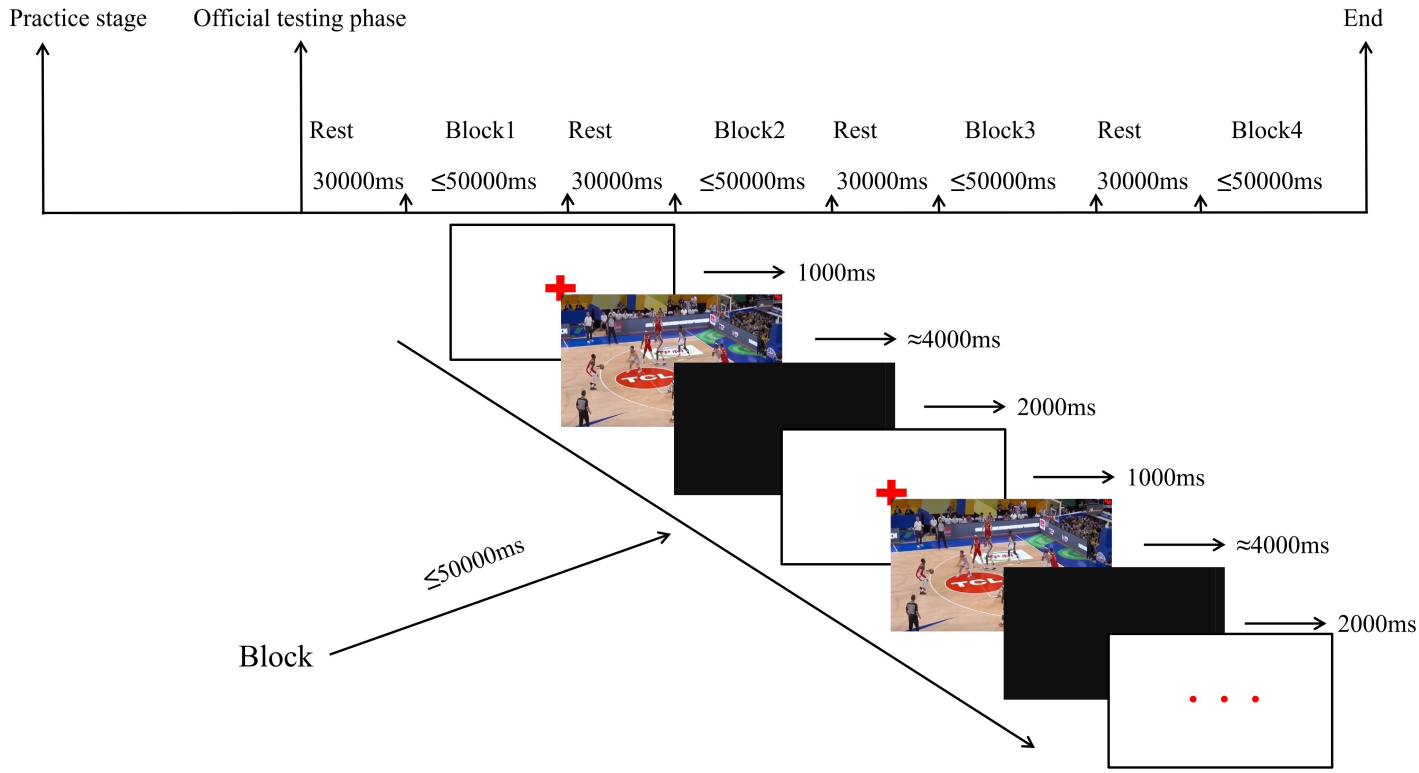
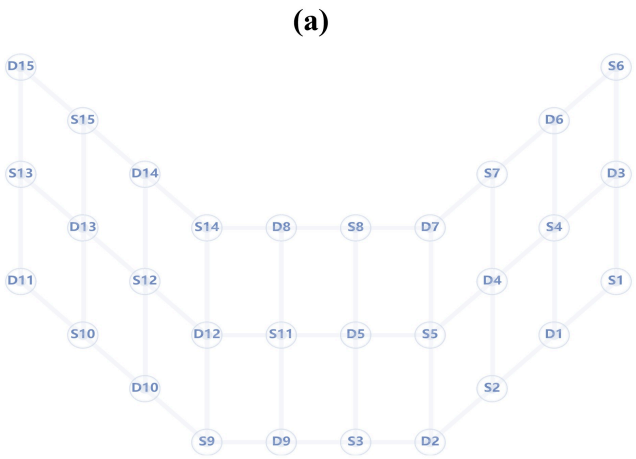


Figure 1

E-prime test paradigm



(b)

ROI Name	Channel Number
DLPFC	3, 7, 22, 26, 32, 35, 40, 41, 42, 44, 45, 46
VLPFC	2, 8, 11, 12, 17, 21, 27, 31, 36
FPA	13, 14, 16, 23, 24, 25, 33, 34, 43
PMC/SMA	1, 9, 18, 20, 30, 37, 39
OFC	4, 5, 6, 15
Other motor sensory areas	10, 19, 28, 29, 38, 47

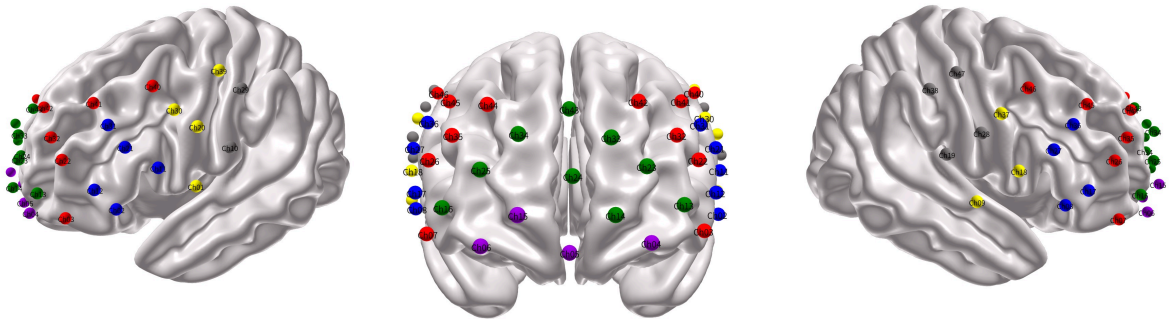


Figure 2

(a) 2D channel layout diagram; **(b)** Table of the specific channel divisions included in each functional ROI. The full names of the five functional brain regions are as follows: DLPFC = dorsolateral prefrontal cortex; VLPFC = ventrolateral prefrontal cortex; FPA = frontal pole area; OFC = orbitofrontal cortex; PMC/SMA = primary motor cortex and supplementary motor area; **(c)** Spatial arrangement of optical poles (emitting and receiving poles) and measurement of channel coverage based on the international 10-20 system.

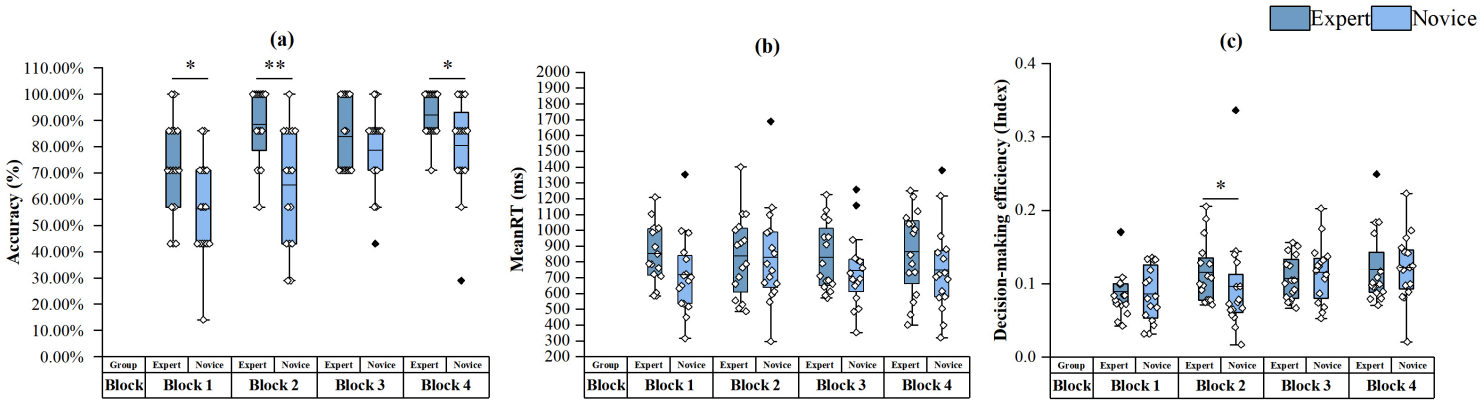


Figure 3

Note: **(a)** Accuracy = decision accuracy (%); **(b)**MeanRT = mean reaction time (milliseconds, ms); **(c)** Decision-making efficiency index. Dark blue boxes represent the expert group, and light blue boxes represent the novice group. The central horizontal line inside the box plot represents the mean, the upper and lower edges of the box represent the upper and lower quartiles (IQRs), respectively, the whiskers extend to the maximum/minimum values within 1.5 times the IQR, and the black diamond-shaped points represent statistical outliers. The superimposed white circles represent the individual true data points of each subject. Differences between groups were compared using either the independent samples *t* test or the Mann–Whitney *U* test based on normality. * p < .05, ** p < .01.

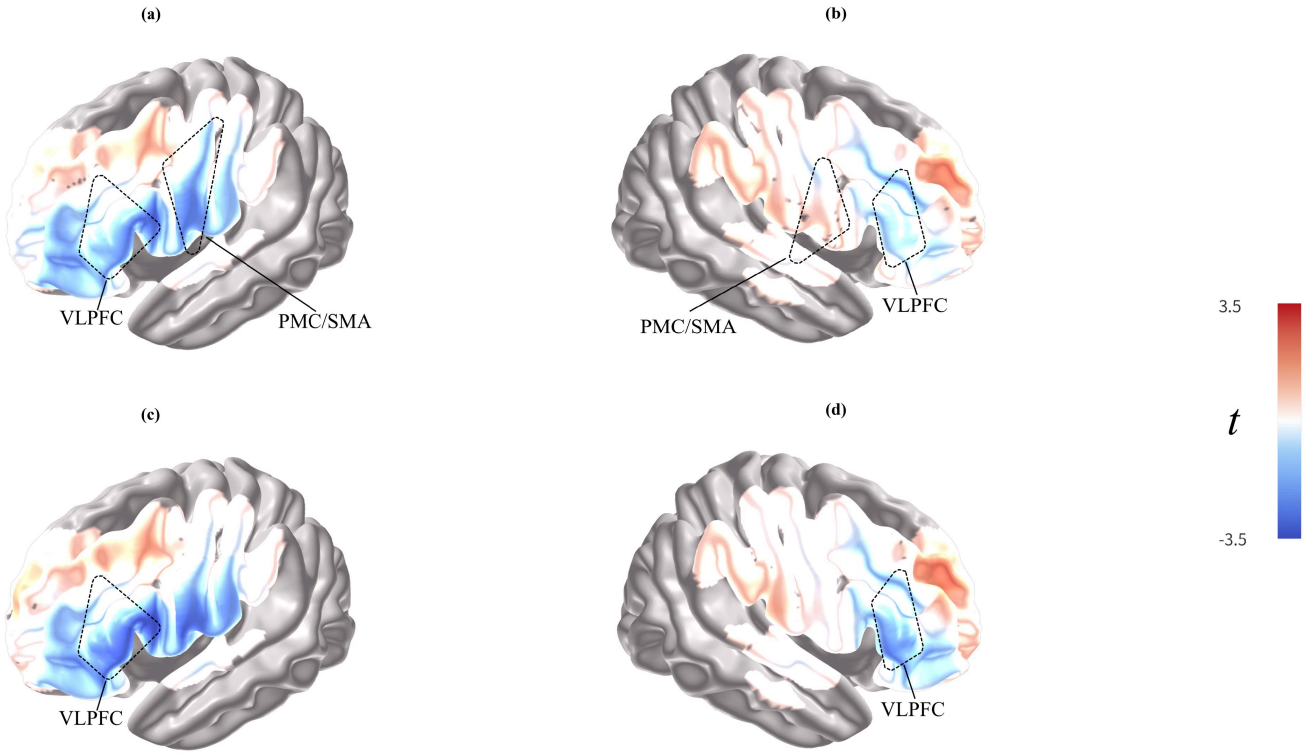


Figure 4

Note: **(a)** and **(b)** show the mapping of differences in mean HbO activation levels (mean) during the task; **(a)** is the left view; **(b)**is the right view; **(c)** and **(d)** show the mapping of differences in peak HbO activation levels (peak) during the task; **(c)** is the left view; **(d)** is the right view. Intergroup differences in brain activation were compared on the basis of independent samples t tests; the color bars represent the range of t values, and the mapping direction is “expert minus novice”. The cool-toned (blue) areas in the figure (such as the VLPFC and PMC/SMA areas) indicate that the HbO activation level in the expert group was significantly lower than that in the novice group.

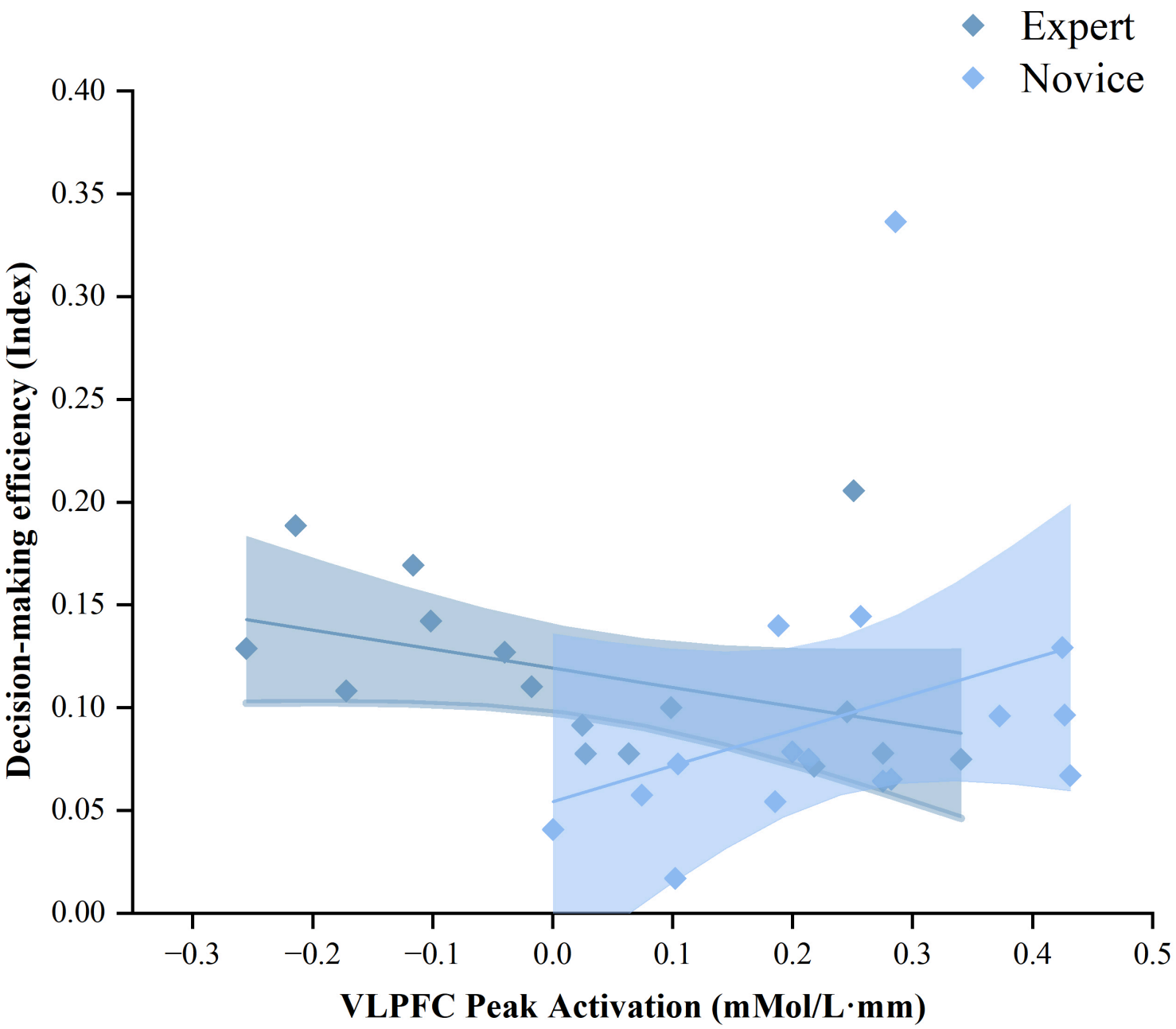


Figure 5

Note: In the figure, the dark blue dots represent individual data from the expert group, and the light blue dots represent individual data from the novice group; the corresponding solid lines and shaded areas represent the linear regression trends and confidence intervals between the peak VLPFC HbO value and decision-making efficiency for the two groups, respectively.

Supplementary Files

This is a list of supplementary files associated with this preprint. Click to download.

- TableS1.docx